Vol. 15, No. 3 (2026): 1152 - 1163 http://dx.doi.org/10.23960/jtepl.v15i3.1152-1163

JURNAL TEKNIK PERTANIAN LAMPUNG

ISSN 2302-559X (print) / 2549-0818 (online)
Journal homepage : https://jurnal.fp.unila.ac.id/index.php/JTP

Optimization of Operating Parameters on the Reduction of Relative Humidity in a Dehumidifier Dryer Using Response Surface Methodology

Iswahyono[1,✉], Yossi Wibisono[2], Didiek Hermanuadi[2], Amal Bahariawan[2], Meta Fitri Rizkiana[3]

[1] Agricultural Engineering, Department of Agricultural Technology, Jember State Polytechnic, Jember, INDONESIA.

[2] Food Engineering Technology, Department of Agricultural Technology, Jember State Polytechnic, Jember, INDONESIA.

[3] Department of Chemical Engineering, Faculty of Engineering, Universitas Jember, Jember, INDONESIA.

Article History:

Received : 25 January 2026
Revised : 17 May 2026
Accepted : 18 May 2026

Keywords:

Dehumidifier dryer,
Relative humidity (RH),
Response surface methodology.

Corresponding Author:
✉ iswahyono@polije.ac.id
(Iswahyono)

ABSTRACT

Relative humidity (RH) of the drying air is the main driving force in the drying process, as dry air has a greater capacity to absorb water vapor from the material; therefore, the lower the RH, the faster the drying rate. This study aims to determine the optimal RH point under varying airflow rate, evaporator temperature, and heater temperature, and to identify the most suitable RSM model equation. The research was carried out in three stages: (1) development of a dehumidifier dryer; (2) optimization and modeling using the Response Surface Methodology (RSM) with three factors—airflow rate, evaporator temperature, and heater temperature—and one primary response, namely the RH of drying air, along with an additional response of drying air temperature. Design Expert v13 software with the RSM Central Composite Design (CCD) was used to select optimum process conditions from the combination of operating parameters. The accuracy of heater temperature control was analyzed using relative error. The relationship between variables and the RH response of air entering the drying chamber was modeled as: $Y = 14.02 + 0.8154A + 0.7625B - 2.75C - 0.4375AB - 0.0875AC - 0.2625BC + 2.48A^2 + 3.09B^2 + 9.83C^2$ (where A = airflow rate, B = evaporator temperature, and C = heater temperature). The optimal RH response of the drying air was 20.263% at an airflow rate of 0.018 m³/s, evaporator temperature of 8.413 °C, and heater temperature of 39.49 °C. Air heating temperature control performed very well, with a relative error of 1.22%, which is below 5%.

1. INTRODUCTION

Drying plays an important role in daily life, particularly in the food sector. In post-harvest handling, drying is essential for various purposes such as preservation and processing of high-moisture products. Drying is defined as the process of removing a portion of water from a material by evaporating most of its moisture content using thermal energy (Mujumdar, 1995). Factors influencing the drying process include drying air temperature, relative humidity, airflow rate, and the material's initial and final moisture content (Asrate & Ali, 2025). These parameters significantly affect both the drying rate and the quality of the dried product (Djaeni & Sari, 2015).

The advantages of drying include extending shelf life and producing materials with smaller volume, which facilitates handling, transportation, and packaging. In addition, reducing material weight simplifies transportation and lowers transportation costs (Wignyanto & Lestari, 2015).

Conventional sun drying is still widely practiced due to its low cost; however, it requires a long drying time and is highly dependent on weather conditions (El-Mesery & El-Khawaga, 2022). Hot air drying, on the other hand, offers a faster drying rate but generally operates at relatively high temperatures, which can cause surface hardening (case

hardening) as moisture inside the material is hindered from evaporating. Moreover, high-temperature drying can damage the physical and chemical properties of heat-sensitive materials. To overcome problems associated with high-temperature drying, drying operations can be conducted at low temperature and low relative humidity using a dehumidification drying system or a dehumidifier dryer (Sudirman *et al*., 2023). The component responsible for reducing air moisture through the dehumidification process is the dehumidifier (Berutu *et al*., 2018).

In a dehumidifier drying system, air undergoes both dehumidification and heating processes. First, dehumidification occurs when air passes through the evaporator, where it is cooled below its dew point. Under these conditions, water vapor in the air condenses into liquid, thereby reducing the air's moisture content. Second, the heating process occurs as the air passes through the condenser, where it absorbs the rejected heat, raising its temperature to near-ambient levels. This process results in a reduction of absolute humidity, enthalpy, wet-bulb temperature, and relative humidity, accompanied by an increase in air temperature (Triyastuti *et al*., 2018). Low relative humidity air provides a strong driving force for mass transfer of moisture from the wet material to the surrounding air, thereby accelerating the evaporation process (Petro *et al*., 2022; Rahmanto *et al*., 2011).

Dehumidifier drying research generally combines air conditioning (AC) systems as cooling and drying units. In such systems, air leaving the evaporator is reheated to temperatures ranging from 30 °C to 57 °C. Increasing heater temperature reduces relative humidity because higher air temperature possesses a greater moisture-holding capacity (Gomez *et al*., 2023). At relatively constant moisture content, higher air temperature lowers RH, enhances the vapor pressure gradient between the drying air and the material surface, and increases both heat transfer and moisture diffusivity during drying (He *et al*., 2021). Low relative humidity further facilitates moisture removal from the material. In addition, airflow rate influences RH by continuously removing humid air from the drying chamber and replacing it with drier air, thereby improving convective heat and mass transfer during drying (Defraeye, 2014). Compared to conventional dryers, dehumidifier dryers offer several advantages, including hygienic operation, ease of temperature and humidity control over a wide temperature range (Kodaloglu *et al*., 2023), improved product quality, independence from weather conditions, absence of smoke emissions, and better color and aroma retention compared to high-temperature drying methods.

Modelling and optimization studies of dehumidifier dryers have been conducted by Azis *et al*. (2013), focusing on the effects of variations in heater temperature and airflow rate. The dryer used was developed by integrating an AC unit into a grain drying system to reduce air temperature and relative humidity. The optimal solution within the investigated range of heater temperature and airflow rate was 40 °C and 0.012 m^3/s, respectively. The optimal RH value was 14.918% based on model prediction and 15% based on experimental results, with an error of 0.054%.

A dehumidifier dryer has previously been developed by the proposing research team (Djamila *et al*., 2024a; Djamila *et al*., 2024b). Experimental results demonstrated that low-temperature, low-RH drying conditions successfully produced moringa powder in accordance with Indonesian National Standards (SNI). However, further development is required, including the addition of an inverter-controlled blower for airflow regulation, evaporator temperature control to optimize moisture removal through condensation and maintain effective dehumidification, a defrost system to prevent frost formation on the evaporator during condensation, and heater temperature control before air enters the drying chamber to allow precise adjustment of inlet air temperature.

Based on the aforementioned studies, further development, modelling, and optimization of the dehumidifier dryer are necessary. This research presents novel approaches to dehumidifier dryer development by implementing controlled airflow rate, evaporator temperature control, and heater temperature control. The developed model employs three independent variables—airflow rate, evaporator temperature, and heater temperature before air enters the drying chamber—with one primary response variable, namely drying air relative humidity, and one additional response variable, inlet air temperature. These three variables were selected because they strongly influence the drying air conditions in contact with the material.

Therefore, this study aims to determine the optimal conditions for airflow rate, evaporator temperature, and air heater temperature, and to establish the most suitable Response Surface Methodology (RSM) model equation. The resulting model can be used to identify operating conditions producing the lowest relative humidity while maintaining the drying air temperature close to room temperatures, enabling effective drying of heat-sensitive materials.

2. MATERIALS AND METHODS

2.1. Materials and equipment

This research was conducted from June to November 2025 at the TEFA Alsintan, Department of Agricultural Technology, Politeknik Negeri Jember. The equipment used in this study included: 1) a dehumidifier dryer machine subjected to further development and optimization; 2) an Arduino Mega 2560 microcontroller and DHT22 temperature and humidity sensors; 3) a data logger; 4) an anemometer to measure airflow velocity; 5) a hygrometer to measure air temperature and humidity; 6) thermocouples to measure temperature; 7) electrical sockets as the power supply; and 8) a stopwatch to measure time. The material used in this study was ambient air, which was processed by the dryer through dehumidification, resulting in air with reduced temperature and humidity inside the drying chamber. The evaporator temperature was maintained below ambient temperature through the vapor-compression refrigeration cycle using R-22 refrigerant. This low-temperature refrigerant absorbed heat from the surrounding air, thereby promoting moisture condensation and dehumidification.

2.2. Research method

This study was conducted in two main stages. The first stage involved developing the existing dehumidifier dryer to enable control of airflow rate, evaporator temperature, and heater temperature for optimization. Activities in this stage included the installation of an inverter to regulate airflow rate, the addition of evaporator temperature control and a defrost system to prevent frost formation on the evaporator during condensation, and the installation of an air heater temperature control positioned before the air entered the drying chamber to ensure that the inlet air temperature matched the desired setpoint.

The second stage involved experimental design using Design-Expert v13 software, beginning with the identification of factors affecting the drying air relative humidity (RH). The factors investigated in this study for the developed dryer system were airflow rate (A), evaporator temperature (B), and heater temperature (°C). The experimental design employed a Central Composite Design (CCD) with 20 runs, including 14 treatment combinations and 6 center points. A detailed description of the factors and their corresponding levels is presented in Table 1. In addition to evaluating the RH response to airflow rate, evaporator temperature, and heater temperature, this study also assessed the accuracy of the drying air temperature control. The drying air temperature data were derived from the heater temperature settings; thus, the expected drying air temperature corresponded to the heater setpoint.

Table 1. Determination of factors and levels

Variable	Symbol	Code Level		
		-1	0	1
Airflow rate (m^3/s)	A	0.014	0.0215	0.029
Evaporator temperature (°C)	B	5	7.5	10
Heater temperature (°C)	C	30	35	40

Each factor level was coded as −1 for low, 0 for center, and +1 for high.

2.3. Experimental procedure

The first step of the experiment involved preparing the equipment, including assembling the dehumidifier dryer with the additional heater temperature-control components, followed by operating the system until it was ready for use. Prior to data collection, airflow velocity was measured using an anemometer. The airflow rate was calculated using the relation $Q = Av$, where Q is the airflow rate, A is the cross-sectional area of airflow, and v is the air velocity.

Once the dryer was in operation, the evaporator temperature, heater temperature, and airflow rate were adjusted according to the experimental design variations. Each experimental condition lasted 2 hours, with observations recorded every 20 min. The measured parameters included the RH and temperature of the drying air. After data collection, the RH values were entered into Design-Expert v13 software for response surface analysis and to calculate the error in temperature control performance. The measurement points for RH and air temperature are illustrated in the schematic shown in Figure 1.

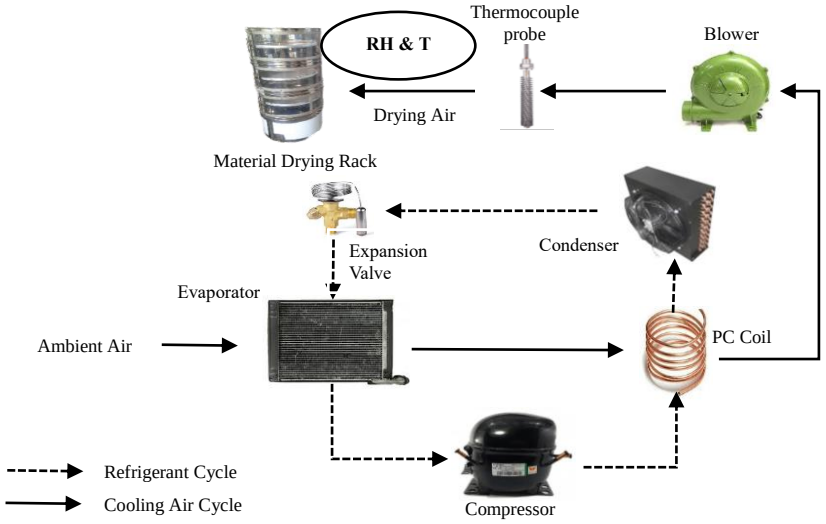

Figure 1. Schematic diagram of drying air RH and temperature measurement in the dehumidifier dryer

2.4. Data analysis

Data processing and analysis were conducted using Design-Expert v13 software. The obtained data were incorporated into a Central Composite Design with a single response, namely relative humidity (RH). The data analysis procedure consisted of the following steps: 1) Model selection, based on the sequential model sum of squares, lack-of-fit test, and model summary statistics. This step aimed to identify the most appropriate model describing the relationship between the factors and the response. 2) Analysis of the selected model, performed using analysis of variance (ANOVA). After determining the most suitable model, ANOVA was used to assess the significance of the relationships among the variables in this study. 3) Three-dimensional (3D) surface and contour analysis, along with the determination of the mathematical model describing the effects of the investigated factor variations. 4) Optimization of the response value and validation of the predicted results against actual experimental data. Validation was conducted by performing three experimental replications under the optimal treatment combination generated by the software (Asrate & Ali, 2025).

The error in temperature control performance was expressed as absolute error, defined as the difference between the heater temperature setpoint and the measured drying air temperature. Alternatively, the error was expressed as a relative error, defined as the ratio of the absolute error to the measured temperature (Saptadi, 2014).

3. RESULTS AND DISCUSSION

3.1. Results of dehumidifier dryer development

This stage aimed to enable control of airflow rate, evaporator temperature, and drying air temperature. The outcomes of the dehumidifier dryer development stage are summarized as follows:

1. Installation of an inverter to control blower speed by adjusting the frequency and voltage supplied to the inverter, thereby allowing the blower speed to be set according to the desired airflow rate.
2. Installation of an STC-3028 thermostat to control the evaporator temperature according to the required setpoint, along with the addition of a defrost system to prevent frost formation on the evaporator during the condensation process.
3. Installation of an air heater and temperature control system using a thermoregulator positioned before the air enters the drying chamber, aimed at controlling the drying air temperature to match the required drying conditions.
4. Installation of a data logging system for monitoring and recording the relative humidity (RH) and temperature of the drying air using Arduino Mega 2560 microcontroller equipped with DHT22 sensors. The measured data were automatically displayed on a 20×4 LCD screen during the experiments and stored in memory for further analysis.

3.2. Modeling and optimization data analysis

3.2.1. ANOVA test

The results of the analysis of the effects of blower airflow rate (A), evaporator temperature (B), and heater temperature (C) on the RH response are presented in Table 2. The RH response values ranged from 11.1% to 40.3%. The terms "morning" and "noon" were used solely to reduce experimental error associated with fluctuations in ambient environmental conditions, rather than as treatment variables. Analysis of variance (ANOVA) was conducted to identify the effects and interactions of process variables on the measured response (Rahmawati *et al*., 2022; Widarsaputra *et al*., 2022). This approach allows the identification of factors that have significant impacts, both individually and in combination, thereby providing a deeper understanding of the system behavior. Based on the ANOVA results in Table 2 and the significance criterion of p-value ≤ α (0.05), the heater temperature showed a significant linear effect on RH, while airflow rate and evaporator temperature influenced RH mainly through their quadratic effects.

Table 2. Experimental results of drying air relative humidity (RH) (%)

Std	Block	Run	Factor A : Airflow Rate (m³/s)	Factor B : Evaporator Temperature (°C)	Factor C : Heater Temperature (°C)	Response RH (%)
3	Morning	1	0.014	10	30	38.2
1	Morning	2	0.014	5	30	37.1
11	Morning	3	0.0215	7.5	35	17.7
8	Morning	4	0.029	10	40	30.7
10	Morning	5	0.0215	7.5	35	17.1
2	Morning	6	0.029	5	30	37.4
7	Morning	7	0.014	10	40	32.5
9	Morning	8	0.0215	7.5	35	18.9
12	Morning	9	0.0215	7.5	35	15.8
5	Morning	10	0.014	5	40	31.1
4	Morning	11	0.029	10	30	38.1
6	Morning	12	0.029	5	40	32.4
13	Noon	13	0.0089	7.5	35	12.1
14	Noon	14	0.0341	7.5	35	18.9
15	Noon	15	0.0215	3.2955	35	14.6
20	Noon	16	0.0215	7.5	35	11.1
17	Noon	17	0.0215	7.5	26.591	40.3
16	Noon	18	0.0215	11.7045	35	19.9
19	Noon	19	0.0215	7.5	35	13.1
18	Noon	20	0.0215	7.5	43.409	32.3

Table 3. Analysis of variance (ANOVA) result for drying air relative humidity (RH)

Source	Sum of Squares	df	Mean Square	*F*-value	*p*-value	
Block	357.42	1	357.42			
Model	1603.64	9	178.18	27.23	< 0.0001	significant
A-Airflow Rate	9.08	1	9.08	1.39	0.2690	
B-Evaporator Temp	7.94	1	7.94	1.21	0.2992	
C-Heater Temp	103.27	1	103.27	15.78	0.0032	
AB	1.53	1	1.53	0.2340	0.6401	
AC	0.0613	1	0.0613	0.0094	0.9250	
BC	0.5513	1	0.5513	0.0842	0.7782	
A^2	88.30	1	88.30	13.49	0.0051	
B^2	137.93	1	137.93	21.08	0.0013	
C^2	1391.49	1	1391.49	212.66	< 0.0001	
Residual	58.89	9	6.54			
Lack of Fit	51.90	5	10.38	5.94	0.0545	not significant
Pure Error	6.99	4	1.75			
Cor Total	2019.95	19				

3.2.2. Lack-of-Fit Test

The lack-of-fit test was performed to evaluate the adequacy of the developed model. The hypotheses used in this test were as follows: H_0, the model does not exhibit lack of fit, and H_1, the model exhibits lack of fit. In the lack-of-fit test (Table 2), the null hypothesis (H_0) is rejected if the p-value is less than the significance level α (0.05). Conversely, if the *p*-value is greater than α, the null hypothesis is accepted. Based on the data in Table 2, the *p*-value for the lack-of-fit test was 0.0545. Since this value is greater than 0.05, it can be concluded that the model does not exhibit lack-of-fit, indicating that the quadratic regression model is adequate.

3.2.3. Regression Equation

Based on data analysis using Design-Expert v13 software and response surface methodology (RSM), a quadratic regression equation was generated to describe the relationship between blower airflow rate (A), evaporator temperature (B), and heater temperature (C) on drying air RH (Table 4). This equation illustrates the contribution of each variable in influencing the RH of the drying air.

$$Y = 14.02 + 0.8154A + 0.7625B - 2.75C - 0.4375AB - 0.0875AC - 0.2625BC + 2.48A^2 + 3.09B^2 + 9.83C^2 \quad (1)$$

Table 4. ANOVA result on the effects of blower airflow rate, evaporator temperature, and heater temperature on drying air RH

Source	Sum of Squares	df	Mean Square	*F*-value	*p*-value	
Mean vs Total	12969.32	1	12969.32			
Block vs Mean	357.42	1	357.42			
Linear vs Block	120.29	3	40.10	0.3900	0.7619	
2FI vs Linear	2.14	3	0.7146	0.0056	0.9994	
Quadratic vs 2FI	**1481.20**	**3**	**493.73**	**75.46**	**< 0.0001**	**Suggested**
Cubic vs Quadratic	22.68	4	5.67	0.7829	0.5819	Aliased
Residual	36.21	5	7.24			
Total	14989.27	20	749.46			

The regression equation and ANOVA results indicate that blower airflow rate (A), evaporator temperature (B), and heater temperature (°C) significantly influence the RH of the drying air, with heater temperature having the most pronounced effect, as indicated by its larger regression coefficient magnitude. The positive quadratic terms (A^2, B^2, C^2) indicate the presence of an optimum operating conditions, at which further changes in operating conditions no longer result in a linear behaviour of RH. Interactions among the variables (AB, AC, BC) suggest that specific combinations of airflow rate, evaporator temperature, and heater temperature can either accelerate or slow down the reduction of drying air RH.

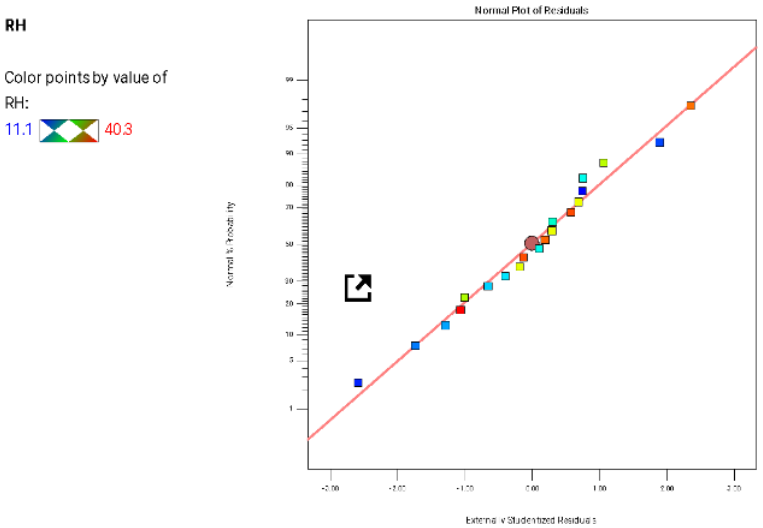

Figure 2. Normal Probability Plot of Residuals

The normal probability plot of residuals (Figure 2), illustrating the relationship between actual and predicted values, shows that the data points are closely distributed along the normal line, indicating that the RH response data are normally distributed. This confirms that the actual experiment results closely match the values predicted by Design-Expert v13. The model can therefore be used to determine optimal operating parameters in the drying process to achieve the desired RH level. Based on the signs and magnitudes of the regression coefficients in the quadratic equation, the RH response decreases with increasing heater temperature, as indicated by the negative coefficient of C, while it increases with increasing airflow rate and evaporator temperature, as indicated by the positive coefficients of A and B.

Based on Table 5, the coefficient of determination (R^2) value of 96.46% indicates that the drying air RH is strongly influenced by blower airflow rate, evaporator temperature, and heater temperature. The remaining 3.54% of the variation is attributed to other factors not considered in this study. The coefficient of determination (R^2) ranges from 0 to 100%, and values closer to 100% indicate a better ability of the model to explain the variability of the observed data (Andreyanto & Sulistiyowati, 2025). Predicted R^2 is a measure of the amount of variation in new data explained by the model. The difference between the predicted R^2 and adjusted R^2 values should generally below than 0.20; otherwise, there may be a problem with either the experimental data or the developed model (Nwadike *et al*., 2020). In this study, the difference between the adjusted R^2 and predicted R^2 values was less than 0.20, indicating that the model still possesses acceptable predictive capability for new observations. However, the lower predicted R^2 suggests reduced prediction accuracy compared to the fitting accuracy for the experimental data.

Table 5. Model summary output

Std. Dev.	Mean	C.V. %	R^2	Adjusted R^2	Predicted R^2	Adeq Precision
2.56	25.47	10.05	0.9646	0.9292	0.7770	17.0942

3.2.4. Contour plot and surface plot analysis

At this stage, contour plots and surface plots were analyzed to examine the relationships between the independent variables—blower airflow rate, evaporator temperature, and heater temperature—and the response variable, namely drying air relative humidity (RH). In Figure 3, contour plot analysis was performed using drying air RH as the response parameter. The first analysis was conducted to determine the optimal heater temperature of 35 °C using a contour plot relating blower airflow rate and evaporator temperature. The optimal airflow rate range was 0.018–0.022 m^3/s, while the optimal evaporator temperature ranged from 6.7 to 7.6 °C, resulting in a drying air RH of less than 14%. Subsequently, an analysis was performed at a fixed evaporator temperature of 7.5 °C using a contour plot relating blower airflow rate and heater temperature. The optimal blower airflow rate ranged from 0.0149 to 0.0255 m^3/s, and the heater temperature ranged from 34.9 to 36.5 °C, yielding a drying air RH of approximately 15%. Further analysis was conducted to determine the optimal blower airflow rate of 0.0215 m^3/s using a contour plot relating evaporator temperature and heater temperature. The optimal evaporator temperature ranged from 5.6 to 8.8 °C, and the optimal heater temperature ranged from 34.2 to 37.8 °C, resulting in a drying air RH of approximately 15%. These operating conditions were selected because they were located within the optimum region (blue zone) predicted by the contour plots and provided low RH under stable near-ambient drying conditions.

In Figure 4, surface plot analysis shows that nearly all plots exhibit a concave shape, indicating the presence of an optimum region where the lowest drying air RH is achieved before increasing again at higher or lower factor levels. In the plot relating blower airflow rate and evaporator temperature, the drying air RH decreases with increasing airflow rate and evaporator temperature until reaching a minimum point, after which it increases again. The optimal combination for achieving the lowest drying air RH was estimated at a blower airflow rate of 0.018–0.022 m^3/s and an evaporator temperature of 6.7–7.6 °C.

In the plot relating blower airflow rate and heater temperature, the drying air RH decreases with increasing process conditions, with the optimal combination occurring at a blower airflow rate of 0.0149–0.0255 m^3/s and a heater temperature of 34.9–36.5 °C, which provides a low drying air RH. Finally, in the plot relating evaporator temperature and heater temperature, the minimum drying air RH occurs at an evaporator temperature range of 5.6–8.8 °C and a heater temperature range of 34.2–37.8 °C. Outside these ranges, the drying air RH increases again.

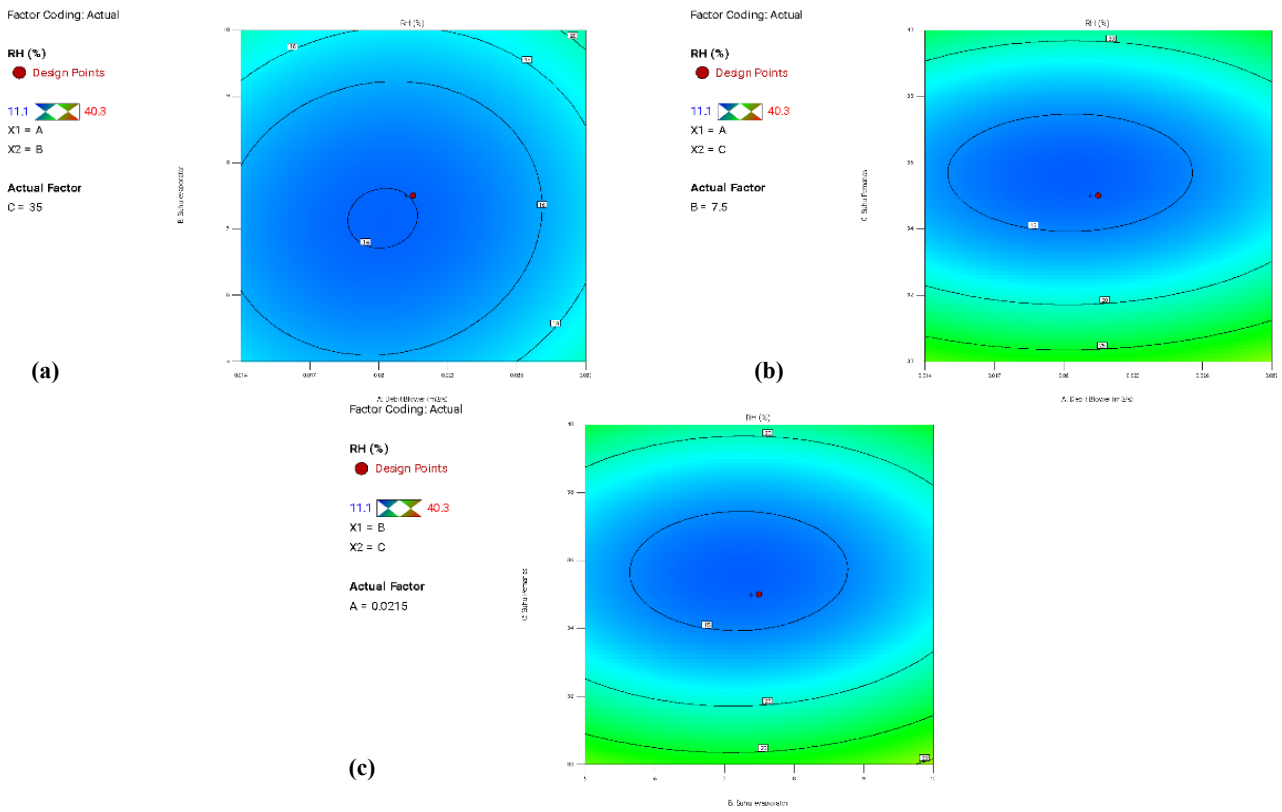

Figure 3. Contour plot of airflow rate, evaporator temperature, and heater temperature optimization on drying air RH.

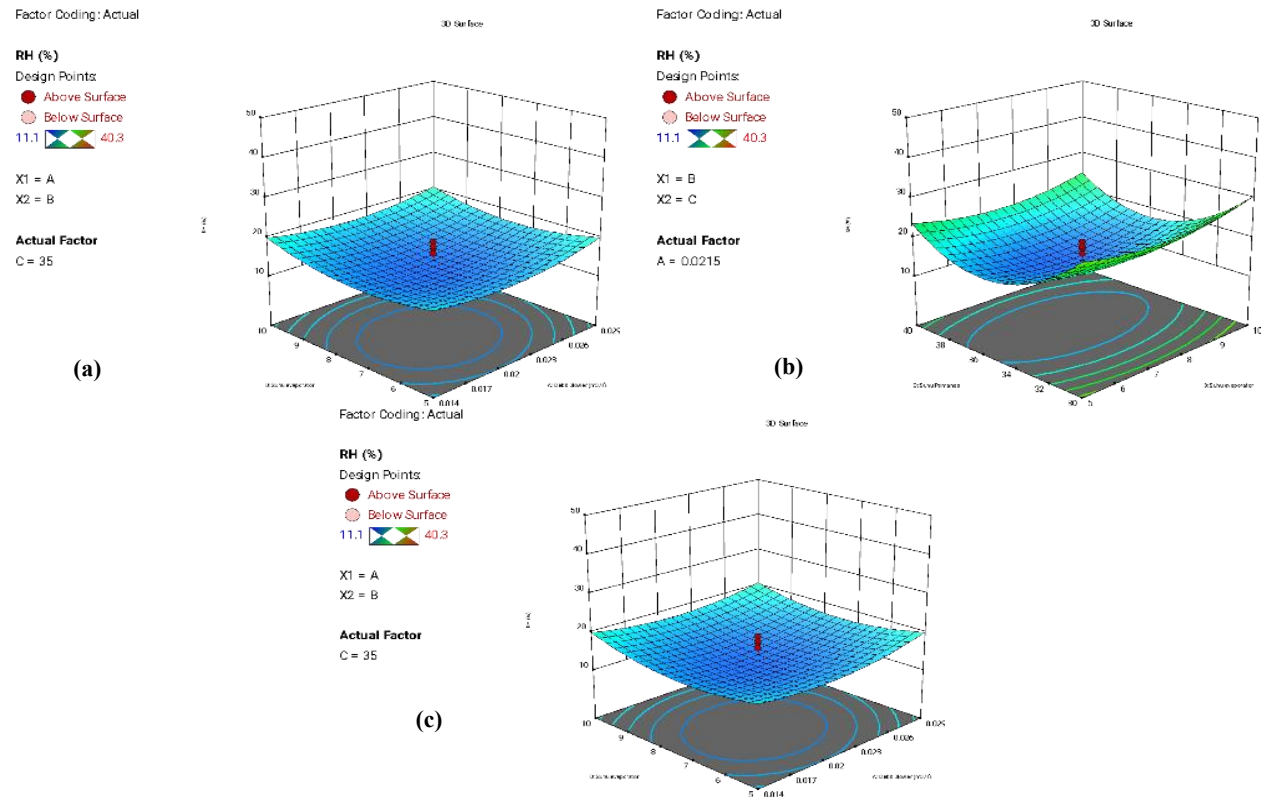

Figure 4. Surface plot of airflow rate, evaporator temperature, and heater temperature optimization on drying air RH

In the plot relating blower airflow rate and heater temperature, the drying air RH decreases with increasing process conditions, with the optimal combination occurring at a blower airflow rate of 0.0149–0.0255 m³/s and a heater temperature of 34.9–36.5 °C, which provides a low drying air RH. Finally, in the plot relating evaporator temperature and heater temperature, the minimum drying air RH occurs at an evaporator temperature range of 5.6–8.8 °C and a heater temperature range of 34.2–37.8 °C. Outside these ranges, the drying air RH increases again.

3.2.5. RSM Optimization

The experimental data collected in this study were further analyzed using Design-Expert v13 software to obtain optimal conditions through the Response Surface Methodology (RSM). This approach enables the identification of patterns and relationships among variables, allowing for a more accurate and efficient determination of optimal solutions.

Based on the RSM optimization results, the optimal operating conditions were an airflow rate of 0.018 m³/s, an evaporator temperature of 8.413 °C, and a heater temperature of 39.490 °C. Under these conditions, the resulting drying air relative humidity (RH) was 20.263%, with a composite desirability value of 1.00, indicating that this combination represents the optimal solution. A desirability value close to 1 signifies a higher capability of the optimization model to achieve the desired response effectively, confirming that the obtained operating conditions are optimal and meet the expected performance criteria (Fauzi *et al.,* 2022; Anwar *et al.*, 2021).

Table 6. Response surface methodology (RSM) optimization of drying air relative humidity (RH) using Design-Expert v13.

Number	Airflow Rate	Evaporator temperature	Heater temperature	RH	Desirability	
1	0.018	8.413	39.490	20.263	1.000	Selected

3.2.6. Confirmation of RSM Optimization Results

The measurement object in this validation was the relative humidity (RH) of the drying air. Validation was conducted through three experimental replications using the optimal combination of blower airflow rate of 0.018 m³/s, evaporator temperature of 8.413 °C, and heater temperature of 39.490 °C. The measured RH values obtained from these experiments were compared with the RSM-predicted results to evaluate the adequacy of the developed model. Based on Table 7, the measured drying air RH values closely matched the RSM prediction results. This finding is further supported by statistical analysis using a one-sample *t*-test, which yielded a *p*-value of 0.545 > Sig. (0.05), indicating that there is no significant difference between the RSM-predicted optimization results and the experimental outcomes.

Table 7. Experimental results for confirmation of the RSM model

Airflow Rate (m³/s)	Evaporator Temp (°C)	Heater Temp (°C)	RH Experimental Test (%)		
			1	2	3
0.018	8.413	39.490	20.45	19.74	20.16

3.2.7. Accuracy test of drying air temperature heater control

The drying air temperature was controlled using a thermoregulator to maintain the desired drying air temperature. The thermoregulator operates by detecting the actual temperature, comparing it with the desired temperature setpoint, and then controlling the heating or cooling element to maintain a constant temperature through a feedback mechanism. The temperature sensor used in this study was a DHT-type thermocouple sensor. Control accuracy was evaluated by determining the deviation between the temperature setpoint and the actual measured temperature, which can be expressed as either absolute error or relative error. The calculated absolute and relative errors are presented in Table 8. The results show an average relative error of 1.22%, which is below the acceptable threshold of 5%, indicating that the heater temperature control performance is very good.

Table 8. Relative error of dryer air heating temperature control result

Run	Block	Airflow Rate m³/s	Evaporator Temp (°C)	Setting Heater Temp (°C)	Drying Air Temp	Error	Relative Error
1	Morning	0.014	10	30	30	0.000	0.000
2	Morning	0.014	5	30	29.8	0.200	0.671
3	Morning	0.0215	7.5	35	34.6	0.400	1.156
4	Morning	0.029	10	40	39.2	0.800	2.041
5	Morning	0.0215	7.5	35	34.3	0.700	2.041
6	Morning	0.029	5	30	30.4	0.400	1.316
7	Morning	0.014	10	40	39.8	0.200	0.503
8	Morning	0.0215	7.5	35	35.2	0.200	0.568
9	Morning	0.0215	7.5	35	35	0.000	0.000
10	Morning	0.014	5	40	39.6	0.400	1.010
11	Morning	0.029	10	30	30.5	0.500	1.639
12	Morning	0.029	5	40	40	0.000	0.000
13	Noon	0.00888655	7.5	35	34.8	0.200	0.575
14	Noon	0.0341134	7.5	35	35.2	0.200	0.568
15	Noon	0.0215	329.552	35	34.8	0.200	0.575
16	Noon	0.0215	7.5	35	34.4	0.600	1.744
17	Noon	0.0215	7.5	26.591	28.6	2.009	7.024
18	Noon	0.0215	117.045	35	34.5	0.500	1.449
19	Noon	0.0215	7.5	35	35.2	0.200	0.568
20	Noon	0.0215	7.5	43.409	43	0.409	0.951
	Average					0.406	1.220

4. CONCLUSIONS

Based on the RSM–CCD design, airflow rate, evaporator temperature, and heater temperature were found to have significant effects on the drying air relative humidity (RH). The relationship between the variables and the RH response of air entering the drying chamber was modeled as: $Y= 14.02 + 0.8154A + 0.7625B - 2.75C - 0.4375AB - 0.0875AC - 0.2625BC + 2.48A^2 + 3.09B^2 + 9.83C^2$, where A is the blower airflow rate, B is the evaporator temperature, and C is the heater temperature. Among the three operating conditions, heater temperature showed the most significant influence based on the magnitude of its regression coefficient in the above quadratic model and its lowest *p*-value (0.0032) among the investigated parameters. The optimal RH response of the drying air entering the drying chamber was 20.263% at an airflow rate of 0.018 m³/s, an evaporator temperature of 8.413 °C, and a heater temperature of 39.49 °C. The heating temperature control performance was very good, with a relative error of 1.22%, which is below the acceptable limit of 5%.

ACKNOWLEDGMENTS

The authors would like to express their sincere gratitude to the Ministry of Higher Education, Science, and Technology, through the DIPA of the Jember State Polytechnic for providing financial support for this research under Grant No. 0940/PL17.4/PG/2025. We also extend our appreciation to Department of Agricultural Technology, Jember State Polytechnic, for providing laboratory facilities and technical assistance.

AUTHOR CONTRIBUTION STATEMENT

Author	C	M	So	Va	Fo	I	R	D	O	E	Vi	Su	P	Fu
Isw	✓	✓	✓	✓	✓	✓		✓	✓	✓			✓	
YW		✓			✓	✓		✓	✓	✓	✓	✓		
DH	✓		✓	✓			✓			✓	✓		✓	✓
AB		✓	✓	✓			✓			✓	✓		✓	✓
MFR					✓		✓			✓		✓		✓

C: Conceptualization
M: Methodology
So: Software
Va: Validation
Fo: Formal Analysis
I: Investigation
D: Data Curation
R: Resources
O: Writing - Original Draft
E: Writing - Review & Editing
Vi: Visualization
Su: Supervision
Fu: Funding Acquisition
P: Project Administration

REFERENCES

Andreyanto, M.F., & Sulistiyowati, W. (2025). Optimizing shrimp cracker production using response surface methodology and root cause analysis to improve quality. *Proceedings UMSIDA*. https://doi.org/10.21070/ups.7658

Anwar, K., Istiqamah, F., & Hadi, S. (2021). Optimasi suhu dan waktu ekstraksi akar pasak bumi (*Eurycoma longifolia* jack.) menggunakan metode RSM (response surface methodology) dengan pelarut etanol 70%. *Jurnal Pharmascience*, ***8***(1), 53-64. https://doi.org/10.20527/jps.v8i1.9085

Asrate, D.A., & Ali, A.N. (2025). Review on the recent trends of food dryer technologies and optimization methods of drying parameters. *Applied Food Research*, ***5***(1), 100927. https://doi.org/10.1016/j.afres.2025.100927

Aziz, M.G.S., Susilo, B., & Sutan, S.M. (2013). Pemodelan dan optimasi variasi suhu dan debit terhadap penurunan nilai relative humidity pada mesin pengering sistem dehumidifier menggunakan respon surface methodology (RSM). 1–11. Accessed on 09 June 2026 from: https://www.scribd.com/document/504890550

Berutu, R., Immanuel, S., Heryanto, A., Nasution, A.H., & Setyawan, E.Y. (2018). Alat pengering pakaian portable dengan memanfaatkan energi panas buangan AC split 1 PK. *Jurnal Flywheel*, ***9***(2), 24–29.

Defraeye, T. (2014). Advanced computational modelling for drying processes – A review. *Applied Energy*, ***131***, 323–344. https://doi.org/10.1016/j.apenergy.2014.06.027

Djaeni, M., & Sari, D.A. (2015). Low temperature seaweed drying using dehumidified air. *Procedia Environmental Sciences*, ***23***, 2–10. https://doi.org/10.1016/j.proenv.2015.01.002

Djamila, S., Bahariawan, A., Warsito, H., Nuruddin, M., & Iswahyono. (2024). Design and performance test of a fluidized bed dryer using dry cold air flow for drying marungga leaves. *IOP Conference Series: Earth and Environmental Science*, ***1338***, 012003. https://doi.org/10.1088/1755-1315/1338/1/012003

Djamila, S., Iswahyono, Wibisono, Y., Hermanuadi, D., Supriyono, Bahariawan, A., Faizin, M.A., & Sakdiya, S.A. (2024). Performance of a drying machine utilizing an air dehumidification process for marungga leaves and identification of marungga flour. *International Journal of Technology, Food and Agriculture*, ***1***(3), 134–143. https://doi.org/10.25047/tefa.v1i3.5606

El-Mesery, H.S., & El-Khawaga, S.E. (2022). Drying process on biomass: Evaluation of the drying performance and energy analysis of different dryers. *Case Studies in Thermal Engineering*, ***33***, 101953. https://doi.org/10.1016/j.csite.2022.101953

Fauzi, R.A., Widyasanti, A., Perwitasari, S.D.N., & Nurhasanah, S. (2022). Optimasi proses pengeringan terhadap aktivitas antioksidan bunga telang (*Clitoria ternatea*) menggunakan metode respon permukaan. *Jurnal Teknologi Pertanian*, ***23***(1), 9–22. https://doi.org/10.21776/ub.jtp.2022.023.01.2

Gomez, R.S., Gomes, K.C., Gurgel, J.M., Alves, L.B., Queiroga, R.A., Magalhães, H.L.F., Pinheiro, L.S.S., Silva, E.J.C., Oliveira, D.S., Moreira, H.W.D., Brito, H.C., Delgado, J.M.P.Q., & Lima, A.G.B. (2023). the effect of air relative humidity on the drying process of sanitary ware at low temperature: An experimental study. *Processes*, ***11***(11), 3112. https://doi.org/10.3390/pr11113112

He, C., Wang, H., Yang, Y., Huang, Y., Zhang, X., Arowo, M., Ye, J., Zhang, N., & Xiao, M. (2021). Drying behavior and kinetics of drying process of plant-based enteric hard capsules. *Pharmaceutics*, ***13***(3), 335. https://doi.org/10.3390/pharmaceutics13030335

Kodaloglu, A.F., Elbir, A., & Sahin, M.E. (2023). Wool drying process in heat-pump-assisted dryer by fuzzy logic modelling. *Thermal Science*, ***27***(4 Part B), 3043–3050. https://doi.org/10.2298/TSCI2304043A

Mujumdar, A.S. (Ed.). (1995). *Handbook of industrial drying* (2nd ed., rev. and expanded). CRC Press. https://doi.org/10.1201/9780429289774

Nwadike, E.C., Abonyi, M.N., Nwabanne, J.T., & Ohale, P.E. (2020). Optimization of solar drying of blanched and unblanched aerial yam using response surface methodology. *International Journal of Trend in Scientific Research and Development (IJTSRD)*, ***4***(3), 659–666.

Petro, P., Danial, D., & Taufiqurrahman, M. (2022). Desain alat pengering memanfaatkan panas buang alat pengkondisian udara. *JTRAIN: Jurnal Teknologi Rekayasa Teknik Mesin*, ***3***(2), 44–50

Rahmanto, D.E., Subrata, I.D.M., & Sutrisno. (2011). Pemanfaatan panas kondensor AC untuk pengeringan bahan pangan: Studi pengeringan chips kentang. In *Prosiding Seminar Nasional PERHETA 2011* (pp. 187–197). Institut Pertanian Bogor.

Rahmawati, I., Fachri, B.A., Nurtsulutsiyah, N., Manurung, Y.H., Reza, M., Palupi, B., Rizkiana, M.F., & Amini, H.W. (2022). Penerapan response surface methodology dalam optimasi kondisi proses ekstraksi antosianin pada limbah kulit kakao dengan metode maserasi menggunakan pelarut etanol. *JC-T (Journal Cis-Trans): Jurnal Kimia dan Terapannya*, ***6***(1), 24–31. https://doi.org/10.17977/um0260v6i12022p024

Saptadi, A.H. (2014). Perbandingan akurasi pengukuran suhu dan kelembaban antara sensor DHT11 dan DHT22: Studi komparatif pada platform ATMEL AVR dan Arduino. *Jurnal INFOTEL*, ***6***(2), 49–56.

Sudirman, S., Baliarta, I.N.G., Sudana, I.M., Arsana, M.E., Nizhami, A.A., & Apriandi, N. (2023). Aplikasi cooling dehumidification pada mesin pengering untuk mengeringkan hasil panen tanaman herbal. *Jurnal Rekayasa Mesin*, ***18***(1), 37–44. https://doi.org/10.32497/jrm.v18i1.4094

Triyastuti, M.S., Finarianingrum, T., & Octaviani, T. (2018). Validasi model pada pengeringan batch pada wortel. *Jurnal Teknik: Media Pengembangan Ilmu dan Aplikasi Teknik*, ***17***(1), 48–53. https://doi.org/10.26874/jt.vol17no1.55

Widarsaputra, A.Y., Prawatya, Y.E., & Sujana, I. (2022). Response surface methodology (RSM) untuk optimasi pengolahan keripik nanas menggunakan mesin vacuum frying. *INTEGRATE: Industrial Engineering and Management System*, ***6***(2), 70–77.

Wignyanto, & Lestari, E. (2015). Application of mechanical dryer for strengthening of production capability of "potato crackers" industry to fulfill market demand. Journal of Innovation and Applied Technology, ***1***(1), 75–81. https://doi.org/10.21776/ub.jiat.2015.001.01.11